

P O L S K A A K A D E M I A N A U K

I N S T Y T U T M A S Z Y N P R Z E P Ł Y W O W Y C H

**TRANSACTIONS
OF THE INSTITUTE OF
FLUID-FLOW MACHINERY**

PRACE

I N S T Y T U T U M A S Z Y N P R Z E P Ł Y W O W Y C H

106



GDAŃSK 2000

THE TRANSACTIONS OF THE INSTITUTE OF FLUID-FLOW MACHINERY

exist for the publication of theoretical and experimental investigations of all aspects of the mechanics and thermodynamics of fluid-flow with special reference to fluid-flow machines

*

PRACE INSTYTUTU MASZYN PRZEPLYWOWYCH

poświęcone są publikacjom naukowym z zakresu teorii i badań doświadczalnych w dziedzinie mechaniki i termodynamiki przepływów, ze szczególnym uwzględnieniem problematyki maszyn przepływowych

Wydanie publikacji zostało dofinansowane przez PAN ze środków DOT uzyskanych z Komitetu Badań Naukowych


EDITORIAL BOARD – RADA REDAKCYJNA

ZBIGNIEW BILICKI * BRUNON GROCHAL * JAN KICIŃSKI
JAROSŁAW MIKIELEWICZ (CHAIRMAN – PRZEWODNICZĄCY)
JERZY MIZERACZYK * WIESŁAW OSTACHOWICZ
WOJCIECH PIETRASZKIEWICZ * ZENON ZAKRZEWSKI

EDITORIAL COMMITTEE – KOMITET REDAKCYJNY

JAROSŁAW MIKIELEWICZ (EDITOR-IN-CHIEF – REDAKTOR NACZELNY)
ZBIGNIEW BILICKI * JAN KICIŃSKI
EDWARD ŚLIWICKI (EXECUTIVE EDITOR – REDAKTOR)

EDITORIAL OFFICE – REDAKCJA

Wydawnictwo Instytutu Maszyn Przepływowych
Polskiej Akademii Nauk
ul. Gen. Józefa Fiszera 14, 80-952 Gdańsk, skr. poczt. 621,
 (0-58) 341-12-71 wew. 141, fax: (0-58) 341-61-44,
e-mail: esli@imp.gda.pl

ISSN 0079-3205

VITALY GNESIN¹ and ROMUALD RZĄDKOWSKI²

A theoretical model of 3D flutter in subsonic, transonic and supersonic inviscid flow

A three-dimensional nonlinear time-marching method for aeroelastic behaviour of oscillating turbine blade row has been presented. The approach is based on the solution of the coupled fluid-structure problem, where the aerodynamic and structural dynamics equations are integrated simultaneously in time, thus providing the correct formulation of a coupled problem as the interblade phase angle at which stability (instability) would occur is also a part of solution.

The ideal gas flow around multiple interblade passages (with periodicity on the whole annulus) is described by the unsteady Euler equations in conservative form, which are integrated by using the explicit monotonous second-order accurate Godunov-Kolgan finite-volume scheme and moving hybrid H-O (or H-H) grid.

The structural model is based on the 3D and 1D models. In 3D model the mode shapes and natural frequencies have been obtained via standard FE analysis techniques. The 1D blade model applied here is a one-dimensional beam described by an extended beam-theory including all important effects on a rotating blade. The fluid and the structural equations are solved using the direct integration method or the modal superposition method. The fluid-structure model is also presented for a very simple two degree of freedom blade model.

1. Introduction

The trend of improved gas turbine engine design with higher aerodynamic blading and smaller physical size attracts much attention to the aeroelastic behaviour of blades not only in compressors, but also in turbines. Flow-induced turbine and compressor blades oscillations can lead to fatigue failures of a construction and so they represent an important problem of reliability, safety, and

¹Ukrainian National Academy of Sciences, 2/10 Pozharsky St., Kharkov 3, 10046 Ukraine

²Institute of Fluid Flow Machinery, Department of Dynamics of Machines, Fiszerka 14, 80-952 Gdańsk, Poland

operating cost.

The blade vibrations can be stable, as in the case of forced vibrations from upstream flow distortions, or they can be unstable, as in case of self-excited vibrations (flutter) caused by energy exchange between the oscillating blade and a mean flow. Flutter is a self-excited instability resulting from aerodynamic forces induced by blade vibration. Forced response is primarily caused by rotation of the blading in nonuniform incoming flow field. In turbomachinery environments the problem is further compounded by the fact that blades vibrate with a relative phase with respect to each other, the value of which is not necessarily known.

In spite of aeroelasticity phenomena are characterized by the interaction of fluid and structural domains, most prediction methods tend to treat the two domains separately, and they usually assume some critical interblade phase angle, for which the flutter analysis is carried out for a single passage.

The undeniable importance of spatial and nonlinear effects for practical turbomachinery configurations has led to the development of three - dimensional methods. Since the early 1980's a number of time accurate Euler and Navier-Stokes procedures have been developed to predict blade row unsteady flows, where unsteadiness is caused by aerodynamic disturbances at the inflow or outflow boundaries, relative motions between the blade rows, or blade vibrations.

At present, the traditional approach in flutter calculations of a palisade is based on frequency domain analysis [1, 2], where the blade motions are assumed to be harmonic functions of time with a constant phase lag between adjacent blades, and the mode shapes and natural frequencies are obtained from in a vacuum structural computations. This approach ignores the coupling of the fluid and the structure vibration.

More recent approaches, the so-called integrated or coupled methods, link the structural and fluid domains via set of boundary conditions that must be satisfied simultaneously throughout the solution phase. A literature review is beyond the scope of this paper, but a survey of aeroelasticity methods can be found in [3].

In recent times the new approaches based on the simultaneous integration in time of the equations of motion for the structure and the fluid are developed [4-7]. These approaches are very attractive due to the correct formulation of a coupled problem, as the interblade phase angle at which the stability (instability) would occur is a part of solution.

In the present study the simultaneous time integration method has been described to calculate the aeroelastic behaviour for a three-dimensional oscillating blade row in transonic gas flow.

2. Coupled fluid-structure problem formulation

The separate calculation for the fluid problem as well as the structure problem is due to a lack of knowledge of the interaction between unsteady aerodynamics and the vibratory motion of the blades. Aeroelasticity is a multidisciplinary subject combining aerodynamics and structural dynamics. The simultaneous integra-

tion in time of the equations of motion for the structure and the fluid allows to obtain the correct formulation of the energy exchange. The energy exchange can occur through the transfer of energy from flow to the moving blade (self-excited oscillations or flutter) or with dissipation of the vibrating blade energy in the flow field (aerodamping). This phenomenon is the important characteristic of an aeroelastic stability (or instability) of the system.

In order to consider the flutter of the palisade the flow and structural models must be assumed.

3. Fluid model

The 3D unsteady transonic flow of an ideal gas is described by the Euler equations, represented as conservation laws in an arbitrary Cartesian coordinate system, rotating with the constant angular velocity ω :

$$\frac{\partial}{\partial t} \int_{\Omega} \mathbf{f} d\Omega + \oint_{\sigma} \mathbf{F} \cdot \mathbf{n} d\sigma + \int_{\Omega} \mathbf{H} d\Omega = 0,$$

$$\mathbf{f} = \begin{bmatrix} \rho \\ \rho v_1 \\ \rho v_2 \\ \rho v_3 \\ E \end{bmatrix}; \mathbf{F} = \begin{bmatrix} \rho \mathbf{v} \\ \rho v_1 \mathbf{v} + \delta_{1i} p \\ \rho v_2 \mathbf{v} + \delta_{2i} p \\ \rho v_3 \mathbf{v} + \delta_{3i} p \\ (E + p) \mathbf{v} \end{bmatrix}; \mathbf{H} = \begin{bmatrix} 0 \\ \rho a_{e1} - 2\rho\omega v_2 \\ \rho a_{e2} - 2\rho\omega v_1 \\ 0 \\ 0 \end{bmatrix}; \delta_{ji} = \begin{cases} 1j = i \\ 0j \neq i \end{cases} \quad (3)$$

Here p and ρ are the pressure and density; v_1, v_2, v_3 are the velocity components; a_{e1} and a_{e2} are the transfer acceleration projections; $E = \rho \left(\varepsilon + \frac{v_1^2 + v_2^2 + v_3^2 - r^2 \omega^2}{2} \right)$ is the total energy of volume unit; ε is an internal energy of mass unit; r is the distance from the rotation axis.

The above system of equations is completed by the perfect gas state equation

$$p = \varepsilon(\chi - 1),$$

where χ denotes the ratio of the fluid specific heats.

The aerodynamic equations forms a set of mixed elliptic-hyperbolic nonlinear partial differential equations with unknown transition surface shape (where the equation changes its type) and with moving boundaries, which are defined during the calculation process.

The Eq. (3) satisfied initial and boundary conditions in the spatial domain, which are limited by the hub, casing and the inlet and outlet sections. Neither an analytical solution has been found nor even the problem of existence and uniqueness of solution has yet been resolved and there is little hope that this problem will be resolved. Numerical solution of these equation can be found. The estimation of an accuracy of the numerical solution is defined by the difference scheme

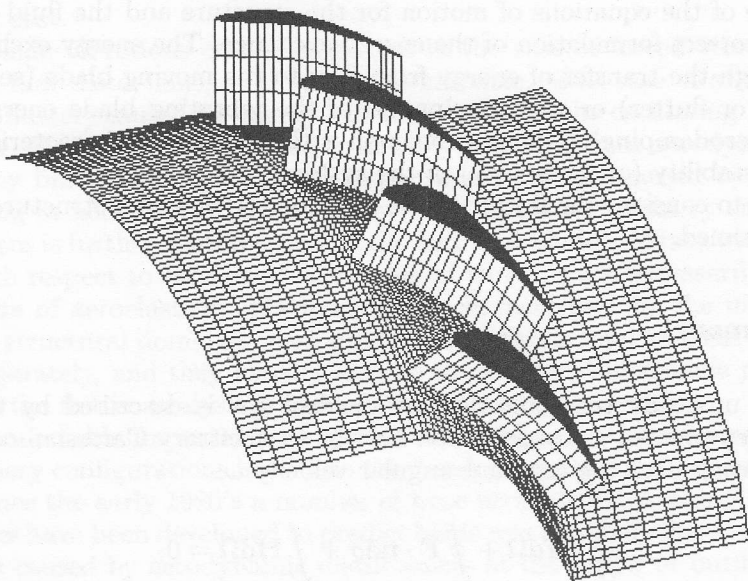


Fig. 1. A view of a sector of the whole blade assembly.

approximation order. The comparison between numerical and experimental results shows how the theoretical predictions are close to the reality.

The physical formulation of the transonic flow through the turbine blade row follows from the fact that this problem does not have a smooth solution, but includes various singularities (discontinuities). Use of the integral conservation laws to construct the difference scheme provides the satisfactory computation of the discontinuous solution without selecting of singularities (so-called through calculation).

3.1. Generalization of Godunov difference scheme for the spatial domain with moving grid

One of an efficient difference scheme known as the Godunov scheme to integrate the hyperbolic equation system has been used for the numerical solution of Eq. (3). This scheme is based on the ideas, which have been developed by Godunov in 1957-1961 [10].

In Godunov's method the conservative variables are considered as piecewise constant over the mesh cells at each time step and the time evolution is determined by the exact solution of the Riemann (shock tube) problem at the inter-cell boundaries. Hence, properties derived from the exact local solution of the Euler equations are introduced in the discretization. This approach has been extended to higher orders, as well as to variants, whereby the local Riemann problem is only approximately solved through approximate Riemann solvers. They are refe-

reed to sometimes as flux difference splitting methods.

It is known that the specific conditions (Hugoniot relations which follow from conservation laws) should be realized on the discontinuity surfaces. These discontinuity could exist as a stable one in an ideal gas flow. So if these necessary conditions are not fulfilled in an initial discontinuity then the discontinuity decomposes into the shock wave, the tangential discontinuity or the expansion wave. Thus the solution of the equation system reduces to the set of discontinuities, which can be calculated relatively simply.

The numerical method based on presented above approach have been widely used to solve of the stationary and non-stationary problems of gas dynamics.

In this paper the 3D unsteady flow through an oscillating turbine blade row with use of Godunov scheme will be considered. The Godunov's scheme has been generalized for the case of three dimensional equations on the moving difference grid.

The calculated domain, includes all blades on the whole annulus, inlet and outlet domains, (see Fig. 2b) and is divided into the finite number of linear hexahedral elements. It is assumed that these elements covers the computational domain. Subdivision of the domain into the hexahedral elements gives the possibility to put them in the right order using indices (i,j,k) (see Fig. 2c).

In the general case, the number of interblade passages, taken into account in the calculation domain, depends on the value of the interblade blade phase angle (IBPA) and is equal to $\frac{2\pi j}{\delta}$, where δ is IBPA (in radians), j is the minimal integer number so that the value $\frac{2\pi j}{\delta}$ is the integer number. The interblade blade phase angle is constant for all blades in the whole annulus.

Computational grid is divided into $\frac{2\pi j}{\delta}$ different passages (see Fig. 2d), each of them includes a blade and has an extension in the circumferential direction, which is equal to the blade pitch. For example, if IBPA is equal to $\delta = \pm\frac{\pi}{2}$, the calculated domain includes four passages (see Fig. 2b). In turn each of the passages is discretized using hybrid H-H or H-O grid (see Fig. 2d). H-grid remains fixed during the calculation, while H(O) grid is rebuilt in each iteration by a presented here algorithm. Hence the external points remain fixed, but internal points (points on the blade surface) move according to the blade motion.

Geometrical and aerodynamical parameters of each passages are described in Cartesian coordinate system x, y, z , fixed rigidly with the static (in equilibrium) position of each blade. Axis x is parallel to the radial direction of a blade, axis z is parallel to the axis of blade rotation, axis y is in the circumferential direction of the cascade, so that the system x, y, z is the right-hand coordinate system (see Fig. 2c).

In the Godunov method the numerical fluxes are obtained from the solution of the Riemann problem in the direction normal (unit normal \mathbf{n}^0) to the elementary cell surface. The position of the normal is defined by three directional cosines of angles (α, β, γ) , between the normal and coordinate axes. It is obvious that the below relation is an identity:

$$|\mathbf{n}^0| = \alpha^2 + \beta^2 + \gamma^2 = 1.$$

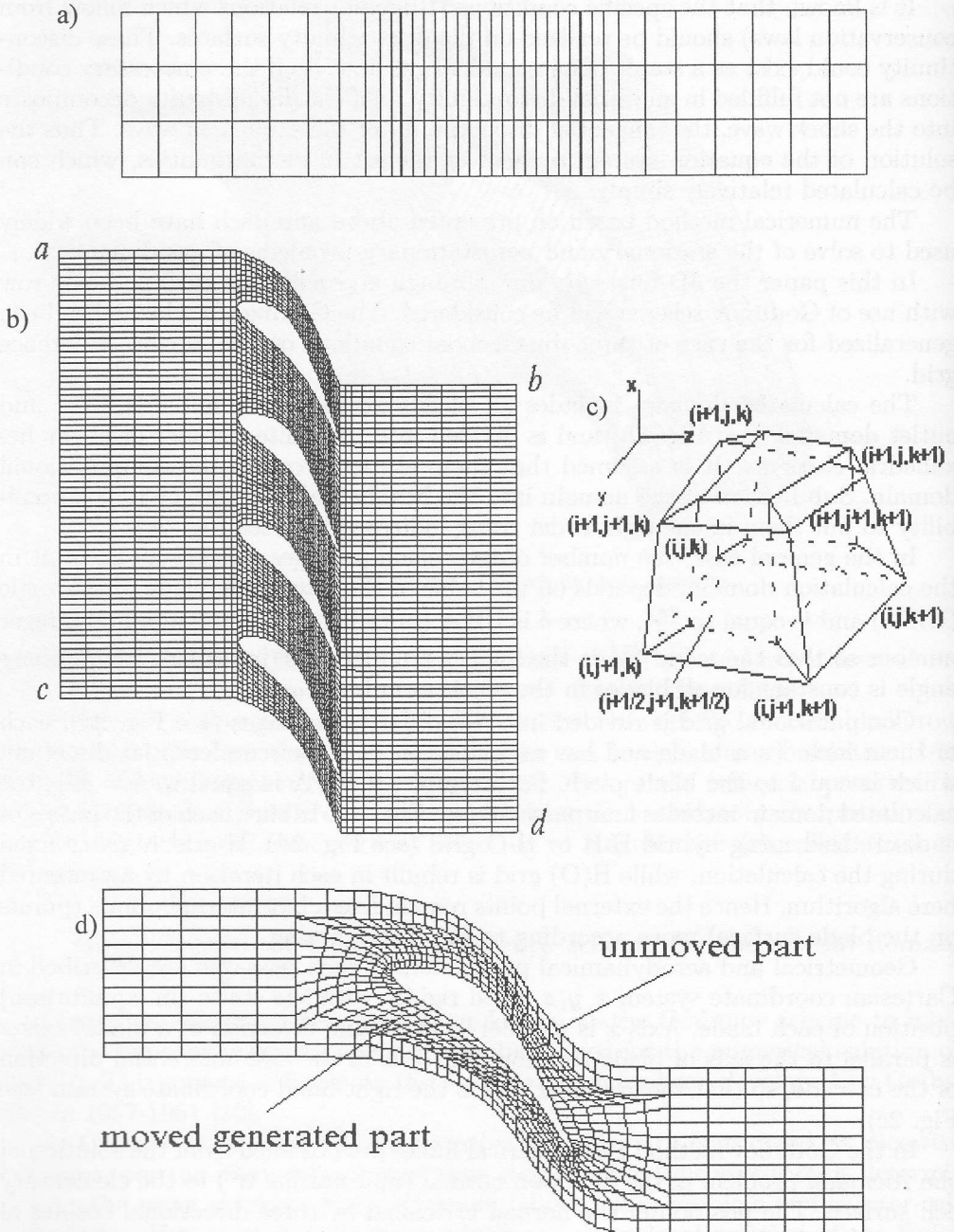


Fig. 2. Hybrid H-H (H-O) – type grid.

Let $\mathbf{n}_1^0 = \{\alpha_1, \beta_1, \gamma_1\}$, $\mathbf{n}_2^0 = \{\alpha_2, \beta_2, \gamma_2\}$, $\mathbf{n}_3^0 = \{\alpha_3, \beta_3, \gamma_3\}$ are external normals to the cell surfaces, which are oriented normally to the axes x, y, z correspondingly. Then symbolic vector of fluxes of density, impulse and energy (see Eq. 3) ($\mathbf{F} \cdot \mathbf{n}^0 = \{\mathbf{F}_1, \mathbf{F}_2, \mathbf{F}_3\}$) can be represented as:

$$\begin{aligned} \mathbf{F}_1 &= \begin{pmatrix} \rho(v_1\alpha_1 + v_2\beta_1 + v_3\gamma_1) \\ \rho v_1(v_1\alpha_1 + v_2\beta_1 + v_3\gamma_1) + p\alpha_1 \\ \rho v_2(v_1\alpha_1 + v_2\beta_1 + v_3\gamma_1) + p\beta_1 \\ \rho v_3(v_1\alpha_1 + v_2\beta_1 + v_3\gamma_1) + p\gamma_1 \\ (E + p)(v_1\alpha_1 + v_2\beta_1 + v_3\gamma_1) \end{pmatrix}, \\ \mathbf{F}_2 &= \begin{pmatrix} \rho(v_1\alpha_2 + v_2\beta_2 + v_3\gamma_2) \\ \rho v_1(v_1\alpha_2 + v_2\beta_2 + v_3\gamma_2) + p\alpha_2 \\ \rho v_2(v_1\alpha_2 + v_2\beta_2 + v_3\gamma_2) + p\beta_2 \\ \rho v_3(v_1\alpha_2 + v_2\beta_2 + v_3\gamma_2) + p\gamma_2 \\ (E + p)(v_1\alpha_2 + v_2\beta_2 + v_3\gamma_2) \end{pmatrix}, \\ \mathbf{F}_3 &= \begin{pmatrix} \rho(v_1\alpha_3 + v_2\beta_3 + v_3\gamma_3) \\ \rho v_1(v_1\alpha_3 + v_2\beta_3 + v_3\gamma_3) + p\alpha_3 \\ \rho v_2(v_1\alpha_3 + v_2\beta_3 + v_3\gamma_3) + p\beta_3 \\ \rho v_3(v_1\alpha_3 + v_2\beta_3 + v_3\gamma_3) + p\gamma_3 \\ (E + p)(v_1\alpha_3 + v_2\beta_3 + v_3\gamma_3) \end{pmatrix}. \end{aligned} \quad (4)$$

Eqs (3) and (4) are not completely divergent (conservative), because of the presence of the constant vector \mathbf{H} in Eq. (3). The reason for this is the noninertiality of the chosen coordinate system, which is rotating with angular velocity ω . When the difference scheme, based on equation system (3), is used, it is important to provide a precise realization of conservation laws of mass, energy and the axial (along z) component of impulse due to the uniformity of corresponding equations. The conservation law of the impulse for radial and angular components are not fully satisfied. If we use the difference approximation for another differential equations forms, all conservation law will not be satisfied.

The general computation algorithm is based on the principle of relaxation over time, i.e. it uses transition from the state in the time moment equal to t_0 to the state in the time moment equal to $t_0 + \tau$.

The discretized form of Eq. (3) was obtained for this transition on an arbitrary moving grid by the Godunov idea [7], but in more universal form extended to three dimensional coordinates.

Let the problem is characterized by the set of parameters at the time t_0 in the grid cells which cover all the calculated domain. The flow parameters in the centre of the cell are given a fractional index $i + 1/2, j + 1/2, k + 1/2$:

$$\{p, \rho, v_1, v_2, v_3\}_{i+\frac{1}{2}, j+\frac{1}{2}, k+\frac{1}{2}} \quad (i = 1, \dots, M; j = 1, \dots, N; k = 1, \dots, L)$$

The parameters at the time t are given a subscript index (i.e. $\rho_{i+1/2, j+1/2, k+1/2}$) as distinct from the parameters at the time $t_0 + \tau$, which are given a superscript

(i.e. $\rho^{i+1/2, j+1/2, k+1/2}$). Here subscripts and superscripts correspond to the points of "old" and "new" grids respectively.

We presuppose that by knowing the given blade motion and using the presented above algorithm of H-H (H-O) – grid generation we can obtain the coordinates $(x^{i,j,k}, y^{i,j,k}, z^{i,j,k})$ and the velocity components of all points at time step τ (the velocity components assume to be constant during the time step):

$$\begin{aligned} \mathbf{w}_{i,j,k} &= \{w_{1i,j,k}, w_{2i,j,k}, w_{3i,j,k}\} \\ x^{i,j,k} &= x_{i,j,k} + w_{1i,j,k} \cdot \tau, \\ y^{i,j,k} &= y_{i,j,k} + w_{2i,j,k} \cdot \tau, \\ z^{i,j,k} &= z_{i,j,k} + w_{3i,j,k} \cdot \tau. \end{aligned} \quad (5)$$

In the moving grid calculation, let us introduce the "middle" side, the coordinates of this side are defined as the half of the sum of the coordinates corresponding to "old" and new grid respectively.

Let $\{\alpha_l, \beta_l, \gamma_l\}$ are the direction cosines of the direction normal to l -th middle cell interface ($l = 1, 2, 3$) and $\{w_{1l}, w_{2l}, w_{3l}\}$ are the velocity components of the middle centre, which can be written as follows

$$\begin{aligned} w_{1l} &= \frac{1}{4} \left(w_{1i,j,k} + w_{1i,j+1,k} + w_{1i,j,k+1} + w_{1i,j+1,k+1} \right), \\ w_{2l} &= \frac{1}{4} \left(w_{2i,j,k} + w_{2i,j+1,k} + w_{2i,j,k+1} + w_{2i,j+1,k+1} \right), \\ w_{3l} &= \frac{1}{4} \left(w_{3i,j,k} + w_{3i,j+1,k} + w_{3i,j,k+1} + w_{3i,j+1,k+1} \right). \end{aligned}$$

Then the velocity of middle cell interfaces centre in the direction of its normal can be written as follows

$$w_{nl} = w_{1l}\alpha_l + w_{2l}\beta_l + w_{3l}\gamma_l \quad (l = 1, 2, 3). \quad (6)$$

Applying the integrals (3) to the moving grid cell (Fig. 2d) with the number $(i + \frac{1}{2}, j + \frac{1}{2}, k + \frac{1}{2})$ during the time integral from t_0 to $t_0 + \tau$, and assuming that velocity of points and gasodynamic parameters on 'middle' cell interface remain constant, the difference analogue of conservation laws was obtained in the form of [7, 9]:

$$\begin{aligned} & \frac{1}{\Delta t} \left[f^{i+\frac{1}{2}, j+\frac{1}{2}, k+\frac{1}{2}} \cdot \Omega_{i+\frac{1}{2}, j+\frac{1}{2}, k+\frac{1}{2}} - f_{i+\frac{1}{2}, j+\frac{1}{2}, k+\frac{1}{2}} \cdot \Omega_{i+\frac{1}{2}, j+\frac{1}{2}, k+\frac{1}{2}} \right] + \\ & + [-(f\sigma w_n)_{i+1} + (f\sigma w_n)_i - (f\sigma w_n)_{j+1} + (f\sigma w_n)_j - (f\sigma w_n)_{k+1} + (f\sigma w_n)_k] + \\ & + [(F_1\sigma)_{i+1} - (F_1\sigma)_i + (F_2\sigma)_{j+1} - (F_2\sigma)_j + (F_3\sigma)_{k+1} - (F_3\sigma)_k] + \\ & + H_{i+\frac{1}{2}, j+\frac{1}{2}, k+\frac{1}{2}} \cdot \Omega_{i+\frac{1}{2}, j+\frac{1}{2}, k+\frac{1}{2}} = 0. \end{aligned} \quad (7)$$

Here subscripts and superscripts correspond to ‘old’ and ‘new’ cells; f are ‘small’ values in cell centres; F_1, F_2, F_3 are ‘big’ values on the ‘middle’ cell interface; σ and w_n are the area and normal velocity of the ‘middle’ cell interface.

The following condition at the discrete realisation of the conservation laws (7) are assumed:

- the “big” values calculated on the “old” cell interfaces transfer without change to the “middle” cell interface;
- the normal velocity w_n of the ‘middle’ cell interfaces and the normal velocity of flow are defined as projections of vectors \mathbf{w} and \mathbf{v} on the normal to the “middle” cell interface.

Taking into account the Eqs (6) and (7) the difference conservation laws of density, momentum and energy for an arbitrary moving cell of calculated domain was written in the following way:

$$\rho^{i+\frac{1}{2},j+\frac{1}{2},k+\frac{1}{2}} = \frac{\Omega_{i+\frac{1}{2},j+\frac{1}{2},k+\frac{1}{2}}}{\Omega^{i+\frac{1}{2},j+\frac{1}{2},k+\frac{1}{2}}} \rho_{i+\frac{1}{2},j+\frac{1}{2},k+\frac{1}{2}} - \frac{\Delta t}{\Omega^{i+\frac{1}{2},j+\frac{1}{2},k+\frac{1}{2}}} \times$$

$$\times \left\{ [(-w_n + v_n)\rho\sigma]_{i+1} - [(-w_n + v_n)\rho\sigma]_i + [(-w_n + v_n)\rho\sigma]_{j+1} - \right.$$

$$\left. - [(-w_n + v_n)\rho\sigma]_j + [(-w_n + v_n)\rho\sigma]_{k+1} - [(-w_n + v_n)\rho\sigma]_k \right\}. \quad (8)$$

$$\left(\rho v_1^{i+\frac{1}{2},j+\frac{1}{2},k+\frac{1}{2}} \right) = \frac{\Omega_{i+\frac{1}{2},j+\frac{1}{2},k+\frac{1}{2}}}{\Omega^{i+\frac{1}{2},j+\frac{1}{2},k+\frac{1}{2}}} (\rho v_1)_{i+\frac{1}{2},j+\frac{1}{2},k+\frac{1}{2}} - \frac{\Delta t}{\Omega^{i+\frac{1}{2},j+\frac{1}{2},k+\frac{1}{2}}} \times$$

$$\times \left\{ \begin{aligned} & [\rho v_1(-w_n + v_n) + \rho\alpha_1]\sigma|_{i+1} - [\rho v_1(-w_n + v_n) + \rho\alpha_1]\sigma|_i + \\ & + [\rho v_1(-w_n + v_n) + \rho\alpha_2]\sigma|_{j+1} - [\rho v_1(-w_n + v_n) + \rho\alpha_2]\sigma|_j + \\ & + [\rho v_1(-w_n + v_n) + \rho\alpha_3]\sigma|_{k+1} - [\rho v_1(-w_n + v_n) + \rho\alpha_3]\sigma|_k - \\ & - [-\rho_{i+\frac{1}{2},j+\frac{1}{2},k+\frac{1}{2}}\omega(2v_{2i+\frac{1}{2},j+\frac{1}{2},k+\frac{1}{2}} + \omega r \cos(\mathbf{r}, x))] \Omega_{i+\frac{1}{2},j+\frac{1}{2},k+\frac{1}{2}} \end{aligned} \right\}. \quad (9)$$

$$\left(\rho v_2^{i+\frac{1}{2},j+\frac{1}{2},k+\frac{1}{2}} \right) = \frac{\Omega_{i+\frac{1}{2},j+\frac{1}{2},k+\frac{1}{2}}}{\Omega^{i+\frac{1}{2},j+\frac{1}{2},k+\frac{1}{2}}} (\rho v_2)_{i+\frac{1}{2},j+\frac{1}{2},k+\frac{1}{2}} - \frac{\Delta t}{\Omega^{i+\frac{1}{2},j+\frac{1}{2},k+\frac{1}{2}}} \times$$

$$\times \left\{ \begin{aligned} & [\rho v_2(-w_n + v_n) + \rho\beta_1]\sigma|_{i+1} - [\rho v_2(-w_n + v_n) + \rho\beta_1]\sigma|_i + \\ & + [\rho v_2(-w_n + v_n) + \rho\beta_2]\sigma|_{j+1} - [\rho v_2(-w_n + v_n) + \rho\beta_2]\sigma|_j + \\ & + [\rho v_2(-w_n + v_n) + \rho\beta_3]\sigma|_{k+1} - [\rho v_2(-w_n + v_n) + \rho\beta_3]\sigma|_k - \\ & - [-\rho_{i+\frac{1}{2},j+\frac{1}{2},k+\frac{1}{2}}\omega(2v_{1i+\frac{1}{2},j+\frac{1}{2},k+\frac{1}{2}} + \omega r \cos(\mathbf{r}, y))] \Omega_{i+\frac{1}{2},j+\frac{1}{2},k+\frac{1}{2}} \end{aligned} \right\}. \quad (10)$$

$$\left(\rho v_3^{i+\frac{1}{2},j+\frac{1}{2},k+\frac{1}{2}} \right) = \frac{\Omega_{i+\frac{1}{2},j+\frac{1}{2},k+\frac{1}{2}}}{\Omega^{i+\frac{1}{2},j+\frac{1}{2},k+\frac{1}{2}}} (\rho v_3)_{i+\frac{1}{2},j+\frac{1}{2},k+\frac{1}{2}} - \frac{\Delta t}{\Omega^{i+\frac{1}{2},j+\frac{1}{2},k+\frac{1}{2}}} \times$$

$$\times \left\{ \begin{aligned} & [\rho v_3(-w_n + v_n) + \rho\gamma_1]\sigma|_{i+1} - [\rho v_3(-w_n + v_n) + \rho\gamma_1]\sigma|_i + \\ & + [\rho v_3(-w_n + v_n) + \rho\gamma_2]\sigma|_{j+1} - [\rho v_3(-w_n + v_n) + \rho\gamma_2]\sigma|_j + \\ & + [\rho v_3(-w_n + v_n) + \rho\gamma_3]\sigma|_{k+1} - [\rho v_3(-w_n + v_n) + \rho\gamma_3]\sigma|_k \end{aligned} \right\}. \quad (11)$$

$$\begin{aligned}
& \left[\rho \left(\frac{1}{k-1} \frac{p}{\rho} + \frac{v_1^2 + v_2^2 + v_3^2 - u^2}{2} \right) \right]^{i+\frac{1}{2}, j+\frac{1}{2}, k+\frac{1}{2}} = \frac{\Omega_{i+\frac{1}{2}, j+\frac{1}{2}, k+\frac{1}{2}}}{\Omega_{i+\frac{1}{2}, j+\frac{1}{2}, k+\frac{1}{2}}} \times \\
& \times \left[\rho \left(\frac{1}{k-1} \frac{p}{\rho} + \frac{v_1^2 + v_2^2 + v_3^2 - u^2}{2} \right) \right]_{i+\frac{1}{2}, j+\frac{1}{2}, k+\frac{1}{2}} - \frac{\Delta t}{\Omega_{i+\frac{1}{2}, j+\frac{1}{2}, k+\frac{1}{2}}} \times \\
& \times \left\{ \begin{aligned}
& \left[\rho \left(\frac{1}{k-1} \frac{p}{\rho} + \frac{v_1^2 + v_2^2 + v_3^2 - u^2}{2} \right) (-w_n + v_n) + p v_n \right] \sigma|_{i+1-} \\
& - \left[\rho \left(\frac{1}{k-1} \frac{p}{\rho} + \frac{v_1^2 + v_2^2 + v_3^2 - u^2}{2} \right) (-w_n + v_n) + p v_n \right] \sigma|_{i+} \\
& + \left[\rho \left(\frac{1}{k-1} \frac{p}{\rho} + \frac{v_1^2 + v_2^2 + v_3^2 - u^2}{2} \right) (-w_n + v_n) + p v_n \right] \sigma|_{j+1-} \\
& \left[\rho \left(\frac{1}{k-1} \frac{p}{\rho} + \frac{v_1^2 + v_2^2 + v_3^2 - u^2}{2} \right) (-w_n + v_n) + p v_n \right] \sigma|_{j+} \\
& + \left[\rho \left(\frac{1}{k-1} \frac{p}{\rho} + \frac{v_1^2 + v_2^2 + v_3^2 - u^2}{2} \right) (-w_n + v_n) + p v_n \right] \sigma|_{k+1-} \\
& - \left[\rho \left(\frac{1}{k-1} \frac{p}{\rho} + \frac{v_1^2 + v_2^2 + v_3^2 - u^2}{2} \right) (-w_n + v_n) + p v_n \right] \sigma|_k
\end{aligned} \right\}. \quad (12)
\end{aligned}$$

The formulas (8-12) characterize the change of density, impulse and energy in the cell in dependence from fluxes of mass, the impulse and the energy through the interface of this cell. The gasodynamic parameters on the lateral sides (expressions in square brackets with integer indexes) are defined using the problem about the break-down (Riemann problem) of an arbitrary discontinuity on the moving interfaces between two adjacent cells and by using of the iteration process.

3.2. The problem about the break-down of an arbitrary discontinuity on the moving side

The description of the difference scheme (8-12) is presented together with the algorithm for calculation of the “big” values (F_1, F_2, F_3), of the fluxes of mass, the impulse and the energy through the lateral sides of difference cell. This algorithm is based on the solution of an auxiliary problem about the break-down of arbitrary discontinuity on the moving side (Riemann problem).

Let α, β, γ are the direction cosines of angles of the normal to the cell interfaces in the direction of x, y, z axes respectively; w_1, w_2, w_3 are the velocity projections of cell interfaces centre on the coordinate axes. Then the normal velocity of the cell interface centre can be written as

$$w_n = w_1 \alpha + w_2 \beta + w_3 \gamma.$$

Let us choose two sets of gasodynamic parameters in two adjacent cells, which have the same interface, and calculate the “big” values on this interface. The signs: + and - denote right and left states across the interface, so the velocity vectors \mathbf{v}^+ and \mathbf{v}^- can be written in terms the normal and the tangential components relatively of the interface

$$\mathbf{v}^\pm = \mathbf{v}_n^\pm + \mathbf{v}_t^\pm,$$

where

$$v_n^\pm = v_1^\pm \alpha + v_2^\pm \beta + v_3^\pm \gamma$$

$$\mathbf{v}_t^\pm = \mathbf{v}^\pm - \mathbf{v}_n^\pm,$$

or through the components

$$\begin{aligned} v_{1n}^\pm &= \alpha v_n^\pm; & v_{2n}^\pm &= \beta v_n^\pm; & v_{3n}^\pm &= \gamma v_n^\pm \\ v_{1t}^\pm &= v_1^\pm - \alpha v_n^\pm; & v_{2t}^\pm &= v_2^\pm - \beta v_n^\pm; & v_{3t}^\pm &= v_3^\pm - \gamma v_n^\pm \end{aligned} \quad (13)$$

To calculate the gasodynamic parameters on the cell boundaries let us use the one-dimensional scheme of the break-down of an arbitrary discontinuity (Riemann problem), following to Godunov [10], [11, p. 159].

As a result of the breakdown of an arbitrary discontinuity three waves were formed, two of them can be the shock wave or the expansion wave, and one of them is the tangential discontinuity. Schematically, the model of the flow structure on the plane can be represented as one of four possible configurations, shown in Fig. 3. The configuration includes the contact discontinuity (CD), in which both the pressure P_{CD} and the tangential velocity component U_{CD} are continuous, but density and the internal energy are discontinuous. In turn these subdomains have been separated from nonperturbed domains with parameters (P^-, ρ^-, v^-) left, and (P^+, ρ^+, v^+) right with the shock wave (SW) or the expansion wave (EW), which are the left or right waves.

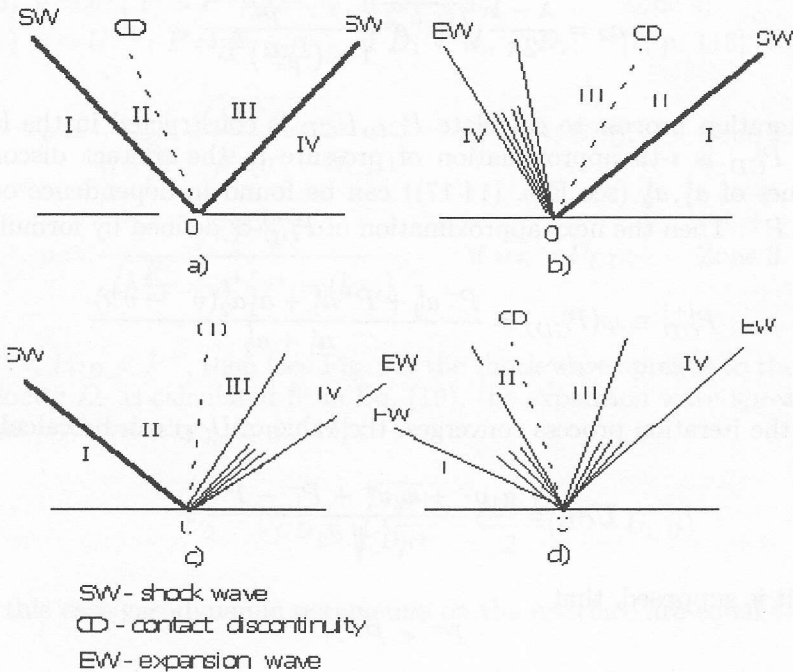


Fig. 3. The break-down of arbitrary discontinuity scheme.

Let us input into consideration the mass velocity of wave [10, p. 108]:

for the "left" shock wave ($P_{CD} \geq P^-$)

$$a_1 = \sqrt{\rho - \frac{(\lambda + 1)P_{CD} + (\lambda - 1)P^-}{2}}, \quad (14)$$

for the "right" shock wave ($P_{CD} \geq P^-$)

$$a_2 = \sqrt{\rho + \frac{(\lambda + 1)P_{CD} + (\lambda - 1)P^+}{2}}, \quad (15)$$

for the "left" expansion wave ($P_{CD} < P^-$) [10, p. 109]

$$a_1 = \frac{\lambda - 1}{2\lambda} \sqrt{\lambda \rho^- \rho^-} \frac{1 - \frac{P_{CD}}{P^-}}{1 - \left(\frac{P_{CD}}{P^-}\right)^{\frac{\lambda-1}{2\lambda}}}, \quad (16)$$

and for the "right" expansion wave ($P_{CD} < P^-$) [10, p. 109]

$$a_2 = \frac{\lambda - 1}{2\lambda} \sqrt{\lambda \rho^+ \rho^+} \frac{1 - \frac{P_{CD}}{P^+}}{1 - \left(\frac{P_{CD}}{P^+}\right)^{\frac{\lambda-1}{2\lambda}}}. \quad (17)$$

The iteration process to calculate P_{CD}, U_{CD} is constructed in the following way. Let P_{CD}^i is i -th approximation of pressure in the contact discontinuity. Then values of a_1^i, a_2^i (see Eqs. (14-17)) can be found in dependence on values P_{CD}^i, P^-, P^+ . Then the next approximation of P_{CD}^{i+1} is defined by formula [10, p. 110]

$$P_{CD}^{i+1} \equiv \varphi(P_{CD}^i) = \frac{P^- a_2^i + P^+ a_1^i + a_1^i a_2^i (v^- - v^+)}{a_1^i + a_2^i}$$

and so on.

After the iteration process converges, the value of U_{CD} can be calculated

$$U_{CD} = \frac{a_1 v^- + a_2 v^+ + P^- - P^+}{a_1 + a_2}. \quad (18)$$

Next it is supposed, that

$$P^- < P^+.$$

This assumption is not a limitation of generality, because the direction of axis and velocity signs can be changed and after the calculation the inverse operation be performed.

In dependence on a value of P_{CD} the following conditions are possible:

1. $P_{CD} > P^+$ and hence $P_{CD} > P^-$.

Then shock waves spread to the left and to the right (see Fig. 3a) with velocities [10, p. 114]

$$D_1 = v^- - \frac{\sqrt{\lambda \frac{P^-}{\rho^-}}}{\rho^-} \quad (\text{left wave}), \quad (19)$$

and [10, p. 115]

$$D_2 = v^+ + \frac{\sqrt{\lambda \frac{P^+}{\rho^+}}}{\rho^+} \quad (\text{right wave}), \quad (20)$$

The considered moving interface can be in one of the zones 1-4 (Fig. 3a), in dependence on values of D_1, D_2, w_n . The gasodynamic parameters on this interface are calculated with the use of the following conditions [10, p. 120]:

- a) $v = v^-; P = P^-; \rho = \rho^-$, if $D_1 \geq w_n$ Zone 1;
 b) $v = v^+; P = P^+; \rho = \rho^+$, if $D_1 \leq w_n$ Zone 4;
 c) $v = U^{CD}; P = P_{CD}$, if $D_1 < w_n < D_2$; [7, p. 115]

$$\rho = \frac{\sqrt{\lambda P^- \rho^-}}{\sqrt{\lambda \frac{P^-}{\rho^-}} - \rho^- (v^- - U_{CD})}, \quad \text{if } w_n < U_{CD}, \quad \text{Zone 2}; \quad (21)$$

$$\rho = \frac{\sqrt{\lambda P^+ \rho^+}}{\sqrt{\lambda \frac{P^+}{\rho^+}} + \rho^+ (v^+ - U_{CD})}, \quad \text{if } w_n > U_{CD}, \quad \text{Zone 3}. \quad (22)$$

2. $P^- < P_{CD} < P^+$, then (see Fig. 3c) the shock wave spreads to the left with velocity D_1 is calculated from Eq. (19), the expansion wave spreads to the right with velocity [10, p. 115]

$$D_2^* = U_{CD} + \sqrt{\lambda \frac{P^+}{\rho^+}} - \frac{\lambda - 1}{2} (v^+ - U_{CD}) \quad (23)$$

In this case gasodynamic parameters on the interface are equal to:

- a) $v = v^-; P = P^-; \rho = \rho^-$, if $D_1 \geq w_n$ Zone 1;
 b) $v = v^+; P = P^+; \rho = \rho^+$, if $D_2^* \leq w_n$ Zone 4;
 c) $v = U^{CD}; P = P_{CD}$, if $D_1 < w_n < D_2^*$; [10, p. 115]

$$\rho = \rho^- \frac{(\lambda + 1)P_{CD} + (\lambda - 1)P^-}{(\lambda - 1)P_{CD} + (\lambda + 1)P^-}, \quad \text{if } w_n < U_{CD}, \quad \text{Zone 2} \quad (24)$$

$$\rho = \frac{\lambda P_{CD}}{[\sqrt{\lambda \frac{P^+}{\rho^+}} - \frac{\lambda - 1}{2}(v^+ - U_{CD})]^2}, \quad \text{if } w_n > U_{CD}, \quad \text{Zone 3} \quad (25)$$

3. $P_{CD} < P_1$ (Fig. 3d). Then expansion waves spread to the left and to the right with velocities [10, p. 115]

$$D_1^* = U_{CD} - \sqrt{\lambda \frac{P^-}{\rho^-}} - \frac{\lambda - 1}{2}(v^- - U_{CD}) \quad (\text{the left wave})$$

and D_2^* is calculated from Eq. (23) for the right wave.

In this case we have :

- a) $v = v^-; P = P^-; \rho = \rho^-$, if $D_1 \geq w_n$ Zone 1;
- b) $v = v^+; P = P^+; \rho = \rho^+$, if $D_2^* \leq w_n$ Zone 4;
- c) $v = U^{CD}; P = P_{CD}$, if $D_1^* < w_n < D_2^*$;

$$\rho = \frac{\lambda P_{CD}}{[\sqrt{\lambda \frac{P^+}{\rho^+}} - \frac{\lambda - 1}{2}(v^- - U_{CD})]^2}, \quad \text{if } w_n < U_{CD}, \quad \text{Zone 2.} \quad (27)$$

If $w_n > U_{CD}$, the wave is in Zone 3, and density is calculated from Eq. (25).

At each cell interfaces, the Riemann problem is solved for some specified pair of left and right states according to the presented above procedure.

As a result we obtain the values of gasodynamic parameters on the interfaces as pressure p , density ρ and the normal component of the total velocity \mathbf{v} . The tangential component of velocity is equal to v_i^- if $w_n < U_{kp}$ or v_i^+ if $w_n < U_{CD}$. The velocity projections on coordinate axes are defined with use of Eqs (13).

Thus the calculation of difference equations (8-12) is reduced to the definition in the explicit form of the gasodynamic parameters \mathbf{f}^{n+1} at the time moment $t = t_n + \Delta t$, for gas dynamic parameters at the moment t_n and values of $(\mathbf{F}_1, \mathbf{F}_2, \mathbf{F}_3)$ calculated with the use of above formulas.

The time step Δt is constant for all calculated domain and is defined from the stability condition of the difference scheme for linearized equation system [10]:

$$\Delta t \leq \frac{\tau_x \cdot \tau_y \cdot \tau_z}{\tau_x \tau_y + \tau_x \tau_z + \tau_y \tau_z}, \quad (28)$$

$$\tau_i = \frac{h_i \min}{\max(u_i + |a|v_i - |a|)}, \quad i = x, y, z$$

where a is the sound velocity.

3.3. Increase of difference scheme accuracy

One of serious requirements imposed on the difference schemes, is their adaptation to the nonregular calculation grids, which can include the cells of different size. The calculated grids for the calculation domains of the complex configuration as a rule include some singularities. The approximation order of the difference scheme decrease in the neighbourhood of these singularities. In order not to lose the approximation order the Kolgan [12] modified the Godunov scheme. The modified Godunov-Kolgan scheme has been applied here.

The Godunov difference scheme uses gasodynamic parameters in the cell centres to calculate the Riemann problem of an arbitrary discontinuity on the cell interface. It supposes that the gasodynamic parameters inside the grid cell are piecewise constant. The Godunov-Kolgan difference scheme supposes piecewise linear distribution of parameters in grid cells. The derivatives used for the linear extrapolation of gasodynamic parameters inside the cell are calculated with the use of minimal value of the derivative principle. In this case the values of parameters inside the cell are defined in the following way:

$$\begin{aligned}
 f(x, y, z) = & f\left(i + \frac{1}{2}, j + \frac{1}{2}, k + \frac{1}{2}\right) + \\
 & + f'_x\left(i + \frac{1}{2}, j + \frac{1}{2}, k + \frac{1}{2}\right) \cdot (x - x_{i+\frac{1}{2}, j+\frac{1}{2}, k+\frac{1}{2}}) + \\
 & + f'_y\left(i + \frac{1}{2}, j + \frac{1}{2}, k + \frac{1}{2}\right) \cdot (y - y_{i+\frac{1}{2}, j+\frac{1}{2}, k+\frac{1}{2}}) + \\
 & + f'_z\left(i + \frac{1}{2}, j + \frac{1}{2}, k + \frac{1}{2}\right) \cdot (z - z_{i+\frac{1}{2}, j+\frac{1}{2}, k+\frac{1}{2}}), \quad (29)
 \end{aligned}$$

where f, f'_x, f'_y, f'_z are the gasodynamic parameters and their derivatives in the direction of axes x, y, x .

To calculate these derivatives, the values of gasodynamic parameters in the centre of considered cell and in centres of six adjacent cells must be known. One set of derivatives f_x^-, f_y^-, f_z^- can be calculated from the system of three linear equations using the parameters increment in cells centres $(i - \frac{1}{2}, j + \frac{1}{2}, k + \frac{1}{2})$, $(i + \frac{1}{2}, j - \frac{1}{2}, k + \frac{1}{2})$, $(i + \frac{1}{2}, j + \frac{1}{2}, k - \frac{1}{2})$ and unknown values of derivatives. For example for the cell with number $(i - \frac{1}{2}, j + \frac{1}{2}, k + \frac{1}{2})$ Eq. (29) can be written:

$$\begin{aligned}
 & f_{i-\frac{1}{2}, j+\frac{1}{2}, k+\frac{1}{2}} - f_{i+\frac{1}{2}, j+\frac{1}{2}, k+\frac{1}{2}} = \\
 & = f_x^-\left(i + \frac{1}{2}, j + \frac{1}{2}, k + \frac{1}{2}\right) \cdot (x_{i-\frac{1}{2}, j+\frac{1}{2}, k+\frac{1}{2}} - x_{i+\frac{1}{2}, j+\frac{1}{2}, k+\frac{1}{2}}) + \\
 & + f_y^-\left(i + \frac{1}{2}, j + \frac{1}{2}, k + \frac{1}{2}\right) \cdot (y_{i-\frac{1}{2}, j+\frac{1}{2}, k+\frac{1}{2}} - y_{i+\frac{1}{2}, j+\frac{1}{2}, k+\frac{1}{2}}) + \\
 & + f_z^-\left(i + \frac{1}{2}, j + \frac{1}{2}, k + \frac{1}{2}\right) \cdot (z_{i-\frac{1}{2}, j+\frac{1}{2}, k+\frac{1}{2}} - z_{i+\frac{1}{2}, j+\frac{1}{2}, k+\frac{1}{2}}). \quad (30)
 \end{aligned}$$

System of Eqs. (30) has an unique solution (f'_x, f'_y, f'_z) when the intervals between cell centres are not parallel. The similar equations can be written for cell centres $(i+1/2, j-1/2, k+1/2)$ and $(i+1/2, j+1/2, k-1/2)$.

The second set of equations with dependence on derivatives f'_x, f'_y, f'_z can be written similarly using the parameter increments in cells $(i+\frac{2}{3}, j+\frac{1}{2}, k+\frac{1}{2})$, $(i+\frac{1}{2}, j+\frac{2}{3}, k+\frac{1}{2})$ and $(i+\frac{1}{2}, j+\frac{1}{2}, k+\frac{2}{3})$.

If one-sided derivatives f^-, f^+ are of the same sign, then the minimal absolute values of considered derivatives must be assumed. In the case of different signs of considered derivatives the derivative equal to zero must be assumed. For example:

$$f'_x = \begin{cases} \min\{|f'_x|, |f'_x|\} \text{sign}(f'_x), & \text{if } f'_x \cdot f'_x > 0; \\ 0, & \text{if } f'_x \cdot f'_x < 0. \end{cases} \quad (31)$$

Such a procedure of choosing the derivatives provides a small 'spreading' of parameters on the interfaces and eliminates the possibility of appearance of the negative pressure values in the linear approximation. Obtained values of derivatives are applied to calculate the parameters at the interface centre (29), which in turn are used to calculate the Riemann problem.

The Godunov-Kolgan scheme presented above is monotonous and has the second order accuracy on the smooth solutions with respect to the spatial coordinates, and has the first order approximation with respect to the time.

To increase the approximation order with respect to the time coordinate it is required that the linear approximation of parameters by spatial coordinates should be completed with the linear approximation at time from the cell centre to the interface centre.

3.4. Initial approximation. Boundary conditions

The steady and unsteady flow calculation for a cascade requires the implementation of different boundary conditions, which determine the solution. These boundary conditions are the kinematic flow condition (vanishing normal velocity at the blade surface), inlet and outlet boundary conditions and periodic boundary conditions at pitchwise boundaries.

As the initial approximation of the unsteady problem, the results of the steady-state calculation were used. Although the strong proof of the correctness of the direct problem formulation does not exist hence only the physical concepts and the experiment can be a criterion to accept the results of the numerical calculation.

On the blade surface, because the grid moves with the blade, the normal relative velocity is set to zero

$$(\mathbf{v} - \mathbf{w}) \cdot \mathbf{n} = 0 \quad (32)$$

It is assumed that the unsteady flow fluctuations are due to prescribed blade motions and the flows far upstream and far downstream from the blade row are

at most small perturbations of uniform free streams. So the boundary conditions formulation is based on the one-dimensional theory of characteristics, where the number of physical boundary conditions depends on the number of characteristics entering the computational domain.

In the general case, when axial velocity is subsonic, at the inlet boundary, initial values for total pressure, total temperature and flow angles are used in terms of the rotating frame of reference, while at the outlet boundary only the static pressure has to be imposed. Nonreflecting boundary conditions can be used, i.e., incoming waves (three at inlet, one at the outlet) have to be suppressed, which is accomplished by setting their time derivative to zero.

The total system of boundary conditions can be represented in the following form:

At inlet [10, p.323], [13]

$$\begin{aligned} T_0 &= T_0(x, y); \quad p_0 = p_0(x, y); \quad \alpha = \alpha(x, y) \\ \gamma &= \gamma(x, y); \quad d(v_3 - \frac{2a}{\lambda-1}) = 0, \end{aligned} \quad (33)$$

at outlet [13]

$$\begin{aligned} p &= p(x, y); \quad dp - a^2 dp = 0; \quad dv_1 - (\omega^2 r - 2\omega v_2) dt = 0 \\ dv_2 + 2\omega v_1 dt &= 0; \quad d(v_3 + \frac{2a}{\lambda-1}) = 0, \end{aligned} \quad (34)$$

where $a = \sqrt{\lambda \frac{p}{\rho}}$ - sound velocity.

In the general case, computations are made using a number of blade passages equal to the number of blades in the cascade. Periodic conditions are applied at the upper and lower boundaries of the calculation domain at each time moment. However there are some situations when it is possible to reduce the number of passages used in the calculations. For unsteady flows, where all blades perform harmonic oscillations with the same mode shape, frequency and a constant interblade phase angle (IBPA) (tuned cascades), the number of blade passages depends on the value of the interblade phase lag. For instance, in the case of computations with the interblade phase angle $\delta = 180$ deg it is sufficient to use two passages, in the case of computations with the interblade phase angles $\delta = 90$ deg, four passages can be used (as shown in Fig. 2a).

The preceding procedure is applicable when the motion of the blades is known in advance. In the time domain method, since the motion of the blades of a coupled fluid-structure problem is not known in advance, it is necessary to include in the numerical calculations all blade passages.

4. Structural model

The structural model is based on the 3D and 1D models. In 3D model, the modes shapes and natural frequencies are being obtained via standard FE analysis techniques. The 1D blade model applied here is a one-dimensional beam described by an extended beam-theory including all important effects on a rotating blade.

The beam is pre-twisted and tapered with the variable cross-sectional area and the stagger angle at the blade root. The model was described in detail in reference (see Rządowski [9, 10]). The disc is modelled by a moderately thick plate theory. The blade and the disc material are modelled as a Hooke's material. Assuming rigidly fixed blades on the disk rim, the displacements \mathbf{u} of any particle of the bladed disc can be found (see Rządowski [9, 10]).

In order to find an approximate solution for the forced vibrations of the bladed disc, the Hamilton principle can be used

$$\delta \int_{t_1}^{t_2} (E - K) dt = \int_{t_1}^{t_2} \delta(W - D) dt, \quad (35)$$

where E and K are elastic and kinetic energies, respectively and δW and δD are the variations of external work and the internal dissipative forces, respectively.

Following the above equations, the equation of motion of the bladed disc for the forced vibration is represented by the equation

$$\mathbf{M}\ddot{\mathbf{u}} + \mathbf{C}\dot{\mathbf{u}} + \mathbf{K}\mathbf{u} = \mathbf{F}, \quad (36)$$

where: \mathbf{M} , \mathbf{C} , \mathbf{K} are the mass, damping and stiffness matrix of the bladed disc, respectively, and \mathbf{F} is the vector of external forces, \mathbf{u} is the general displacement of the system.

The aeroelastic Eq. (36) will be solved by the direct integration methods or the modal analysis method.

In direct integration methods Eq. (36) is written in the form:

$$\mathbf{M}\ddot{\mathbf{u}}_{tm} + \mathbf{C}\dot{\mathbf{u}}_{tm} + \mathbf{K}\mathbf{u}_{tm} = \mathbf{F}_{tm}, \quad (37)$$

and is integrated at a considered point of time $t_m = t_0 + mt$, by a method of the constant average acceleration [18].

For each point of time t_m , the generalised excitation forces \mathbf{F}_{tm} must be calculated from the flow model, for the position of the blades in cascade.

In the time domain method, the equation of motion was integrated in time, by a method of constant average acceleration (Wilson Θ -method). The initial conditions are the steady flowfield and an assumed unsteady forces applied to the blades.

A direct solution of system (36) can be difficult for the large size of the system (bladed disc). This drawback can be efficiently overcome using a linearized modal approach [17, 18].

In the modal approach to the coupled problem, the dynamic model of the oscillating blade in linearized formulation without taking into account of mechanical damping is governed by the matrix equation

$$\mathbf{M}\ddot{\mathbf{u}} + \mathbf{K}\mathbf{u} = \mathbf{F}, \quad (38)$$

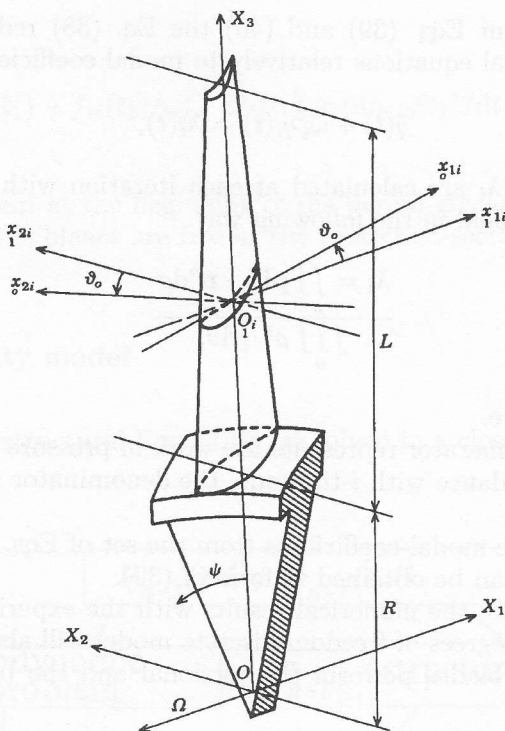


Fig. 4. Model of the bladed disc.

where $\mathbf{u}(x, t)$ and $\ddot{\mathbf{u}}(x, t)$ are respectively blade displacement and acceleration vectors; \mathbf{M} and \mathbf{K} are the mass and stiffness matrices; \mathbf{F} is the vector of unsteady aerodynamic forces, which are a function of blade displacements.

The eigensolution of (38) for $\mathbf{F} = 0$ yields the natural frequencies and the associated mode shapes.

Then the displacement of each blade can be written as a linear combination of the first N mode shapes with the modal coefficients depending on time:

$$\mathbf{u}(x, t) = \mathbf{U}(x, t)\mathbf{x}(t) = \sum_{i=1}^N \mathbf{U}_i(x)q_i(t) \tag{39}$$

where $\mathbf{U}_i(x)$ denotes the i -th mode shape vector, $\mathbf{x}(t)$ are the time dependant modal coordinates.

Functions \mathbf{U} satisfy the orthogonality condition [18]

$$\mathbf{U}^T \mathbf{M} \mathbf{U} = \mathbf{I}, \quad \mathbf{U}^T \mathbf{K} \mathbf{U} = \mathbf{\Omega}^2, \tag{40}$$

where the \mathbf{U} matrix column are the eigenvectors \mathbf{U}_i and $\mathbf{\Omega}^2$ is a diagonal matrix which stores eigenvalues; \mathbf{I} is an identity diagonal matrix.

Taking into account Eqs. (39) and (40) the Eq. (38) reduces to the set of independent differential equations relatively to modal coefficients

$$\ddot{q}(t) + \omega_i^2 q_i(t) = \lambda_i(t), \quad (41)$$

The modal forces λ_i are calculated at each iteration with the use of the instantaneous pressure field in the following way:

$$\lambda_i = \frac{\iint_{\sigma} p \mathbf{U}_i \cdot \mathbf{n}^o d\sigma}{\iint_v \rho \mathbf{U}_i^2 dv}, \quad (42)$$

where p is the pressure.

In Eq. (42) the numerator represents the work of pressure forces at the blade displacement in accordance with i -th mode, the denominator represents the normalising factor.

Having defined the modal coefficients from the set of Eqs. (41), blade displacement and velocity can be obtained in form of (39).

In order to compare the numerical results with the experimental 2D results, the very simple two degrees of freedom discrete model will also be presented.

In this model all blades perform the torsional and the bending oscillations under the given law:

$$h_z(x, t) = h_{z0}(x) \cdot \sin[\omega_h t + (j - 1)\delta],$$

$$h_y(x, t) = h_{y0}(x) \cdot \sin[\omega_h t + (j - 1)\delta],$$

$$\varphi_z(x, t) = \varphi_0(x) \cdot \sin[\omega_\varphi t + (j - 1)\delta],$$

where x, y, z are the Cartesian coordinate system fixed rigidly with j -th blade (origin of coordinates is coincided with the bending centre in the case of the torsional oscillations); $h_z(x, t)$ and $h_y(x, t)$ define the bending oscillations, $\varphi(x, t)$ – the torsional oscillations; $h_{z0}, h_{y0}, \varphi_0$ are the amplitudes of vibration; ω_h is the bending oscillation frequency; ω_φ is the torsional oscillation frequency, δ is IBPA.

The equations of motion of the palisade

$$\ddot{h}_{zi}(t) + \omega_{hi}^2 h_{zi}(t) = f_{zi}(t),$$

$$\ddot{h}_{yi}(t) + \omega_{hi}^2 h_{yi}(t) = f_{yi}(t),$$

$$\ddot{\varphi}_{zi}(t) + \omega_{\varphi i}^2 \varphi_i(t) = m_i(t),$$

were solved for bending and torsion [14, p. 95]. For example in the time interval $(t_1, t_1 + \Delta t)$

$$h_{zi} = (C_2 \sin \omega_h \Delta t + C_1 \sin \omega_h \Delta t) + f_{zi}/\omega_h^2$$

where

$$C_1(t_1) = h_{z_{io}}(t_1) - f_{zi}(t_1)/\omega_h^2, \quad C_2(t_1) = (dh_{z_{io}}(t_1)/dt - f_{zi}(t_1)/\omega_h^2)/\omega_h,$$

$h_{z_{io}}(t_1)$ displacement at the beginning of the period Δt , $\omega_h = 2\pi v_h$.

In this model the blades are free at the root cross-section.

5. Aeroelasticity model

The fluid and the structural Eqs. (1,9) are solved in a closely coupled manner as shown in Fig. 5.

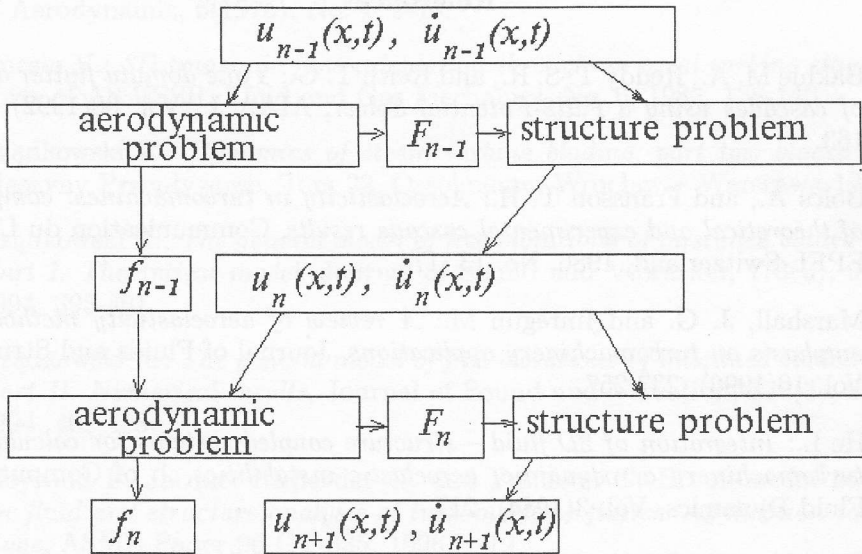


Fig. 5. Computational aeroelasticity program.

The aeroelastic mesh is moved at each time step to ensure correct modelling of the fluid-structure interface.

Here f is a symbol vector of aerodynamic parameters; u, \dot{u} are the blade displacement and velocity; F is the vector of forces distributed on the blade surface.

The time step of calculation is the same for both fluid and structural calculation and is fixed throughout the time integration. A minimum number of 24 time steps per period has been used for the structural modes in order to ensure accuracy of the dynamic method.

6. Conslusions

In the present study, the direct integration method and the modal superposition method is used to determine the aeroelastic stability of the cascade. The unsteady equations of motion for the structure and the fluid are integrated simultaneously in time starting with a steady flowfield and an assumed unsteady forces. Each blade is allowed to move independently and the motion of all blades is analysed to determine the aeroelastic stability of the bladed disc.

The presented time domain method allows a more realistic simulation of the motion of the fluid and the cascade blades that should lead to a better physical understanding.

Received 12 April 2000

References

- [1] Bakhle M. A., Reddy T. S. R., and Keith T. G.: *Time domain flutter analysis of cascades using a Full2-Potential Solver*, AIAA J., Vol. 30(1992), No. 1, 163.
- [2] Bölcs A., and Fransson T. H.: *Aeroelasticity in turbomachines: comparison of theoretical and experimental cascade results*, Communication du LTAT. – EPFL Switzerland, 1986, No. 13, 174.
- [3] Marshall, J. G. and Imregun M.: *A review of aeroelasticity methods with emphasis on turbomachinery applications*, Journal of Fluids and Structures, Vol. 10(1996), 237-257.
- [4] He L.: *Integration of 2D fluid – structure coupled systems for calculation of turbomachinery aerodynamic, aeroelastic instabilities*, J. of Computational Fluid Dynamics, Vol. 3(1984), 217.
- [5] Bendiksen O. O.: *Nonlinear blade vibration and flutter in transonic rotors*, Proc. of ISROMAC-7, The 7th Intern. Symp on *Transport Phenomena and Dynamics of Rotating Machinery*, Feb., 22-26, 1998, Honolulu, Hawaii, USA, 664.
- [6] Chew J. W., Marshall J. G., Vahdati M. and Imregun M.: *Part-speed flutter analysis of a wide-chord fan blade*, T.H. Franson (ed.), *Unsteady Aerodynamics and Aeroelasticity of Turbomachines*, Kluwer Academic Publishers, Printed in the Netherlands, 1998, 707-724.
- [7] Rządkowski R., Gnesin V., Kovalov A.: *The 2D flutter of bladed disc in an incompressible flow*, T.H. Fransson (ed.), *Unsteady Aerodynamics and*

- Aeroelasticity of Turbomachines*, Kluwer Academic Publishers, printed in the Netherlands, 1998, 317-334.
- [8] Sokolovsky G. A., and Gnesin V. I.: *Unsteady and viscous flows in turbomachines*, Naukova Dumka, Kiev, 1986.
- [9] Gnesin V. I. Kolodyazhnaya L. V.: *Numerical modelling of aeroelastic behaviour for oscillating turbine blade row in 3D transonic ideal flow*, Problems in Machinery Engineering, Vol. 1(1999), No. 2, 65-76.
- [10] Godunov S. K. at el: *Numerical solution of multidimensional problems in gasdynamics*, Nauka, Moscow, 1976 (in Russian).
- [11] Chmielniak T.: *The transonic flow*, Maszyny Przepływowe, Tom 16, Ossolineum, Wrocław – Warszawa 1994.
- [12] Kolgan V. P.: *The difference schema for calculation of the two dimensional discontinuous solutions of nonstationary gas dynamics*, Report of the Centre of Aerodynamic, 6(1975), No. 1, 9-14.
- [13] Gnesin V.: *3D transonic flow calculation through an axial turbine stage*, Reports of AS USSR, Fluid and Gas Mechanics, No. 6, 1982, 138-146.
- [14] Rządkowski R.: *Dynamics of steam turbine blading, part two bladed discs*, Maszyny Przepływowe, Tom 22, Ossolineum, Wrocław – Warszawa 1998.
- [15] Rządkowski R.: *The general model of free vibrations of mistuned bladed discs. Part I. Theoretical model*, Journal of Sound and Vibration, 173(3), 9 June 1994, 395-401.
- [16] Rządkowski R.: *The general model of free vibrations of mistuned bladed discs. Part II. Numerical results*, Journal of Sound and Vibration, 173(3), 9 June 1994, 402-413.
- [17] Moyroud F. Jacquet-Richardet G. and Fransson T. H.: *A modal coupling for fluid and structure analysis of turbomachine flutter. Application to a fan stage*, ASME Paper 96-GT-335, 1996, 1-19.
- [18] Bathe K., Wilson E.: *Numerical methods in finite element analysis*, Prentice-Hall, Inc Englewood Cliffs, New Jersey, 1976.

Teoretyczny model trójwymiarowego flatteru niepełnego przepływu poddźwiękowego, transonicznego i ponaddźwiękowego

Streszczenie

Przedstawiono trójwymiarową, nieliniową metodę kroczącą w czasie do badań zachowań aeroelastycznych drgającego szeregu łopatek turbiny. Metoda jest oparta na rozwiązaniu zagadnienia sprzężonego

płyn-wieniec turbiny, gdzie równania opisujące aerodynamikę i dynamikę konstrukcji całkowane są równocześnie w czasie i dlatego przedstawiają właściwy opis zagadnienia sprężonego, gdyż międzyłopatkowy kąt fazowy, dla którego obserwujemy stabilność (niestabilność), jest także częścią rozwiązania.

Przepływ kanałami międzyłopatkowymi gazu doskonałego (z określoną okresowością na całym pierścieniu) jest opisany niestacjonarnymi równaniami Eulera w formie zachowawczej, które są całkowane przy użyciu jawnego schematu drugiego rzędu w formie objętości skończonych Godunowa-Kolgana oraz przemieszczającej się siatki hybrydowej H-O (lub H-H).

Model strukturalny jest oparty na modelach 3D i 1 D. W przypadku modelu 3D częstości własne oraz postacie drgań własnych otrzymywane są przy pomocy standardowych technik elementów skończonych. Jednowymiarowy model łopatki, zastosowany w pracy, jest jednowymiarową belką opisaną przy pomocy rozszerzonej teorii belek, która umożliwia opis wszystkich ważnych efektów wirującej łopatki. Równania płynu oraz konstrukcji rozwiązywane są przy użyciu metody bezpośredniego całkowania lub superpozycji modalnej. Model płyn-konstrukcja jest także pokazany dla przypadku bardzo prostego modelu łopatki o dwóch stopniach swobody.